

RESEARCH

Open Access



Morphology, histology, and chemistry of the wings of *Tribolium castaneum* and *Tribolium confusum* (Coleoptera: Tenebrionidae)

Nasra M.H. Zohry^{1*}  and Ahmed Mohamed El-Sayed²

Abstract

Background: Insect wings are an excessively diverse structures, which have fascinated scientist for centuries. Coleoptera is the largest order in the insect group and the most successful animal on earth (Nature Communications 9(205):1–11, 2018). In order to adapt to the change in the environments, they developed strategies to cope up with different factors. The most distinctive feature of beetles is that the forewings are sclerotized into elytra; from this, they get their formal name (koleos = sheath, pteron = wing). The elytra play an important role in protecting the delicate hindwings and the dorsal surface of the abdomen. Besides its influence on protective the hindwing during flight, the forewings are open enough to allow the hindwings to unfold and function.

Result: The structural and mechanical properties in living organisms may improve the understanding of natural solutions and advance the design of novel artificial materials. In this paper, the morphological and histological structure of the wings of two species of beetles, *Tribolium castaneum* and *Tribolium confusum*, has been investigated using scanning electron microscopy (SEM). The organic chemical function groups of the wings were detected using Fourier-transformed infrared spectroscopy (FTIR). Both *Tribolium* species have considerable variations regarding the total thickness, and width of the hemolymph space within the elytra. The elytra of both species bear conspicuous field of trichoid sensilla from dorsal side and numerous gland openings with a pit. The microtrichia found on the ventral side may have an important role in wing folding. The presence of C–H stretching bands with the prevalence of methylene bands may indicate the presence of long-chain aliphatic acids in surface waxes in *T. castaneum*. The height of the spikes of the hindwings was remarkable by hydrogen-bonded O–H and N–H amide stretching vibration and was correlated to the thickness of the wing.

Conclusion: Insect wings are a core example of histological and morphological novelty. This study illustrates the morphological and histological structure of both the forewing and hindwing of *Tribolium castaneum* and *Tribolium confusum* which were the most destructive pest stored products.

Keywords: Tenebrionidae beetles, Red flour beetle, Flour beetle, Chemical composition, Wing exoskeleton, TEM

* Correspondence: nasramohamed917@gmail.com

¹Department of Zoology, Faculty of Science, Sohag University, Sohag, Egypt
Full list of author information is available at the end of the article

Background

The microstructure of insect wings had been reported to help improve the design and fabrication of bionic wings (Ha, Truong, Phan, Goo, & Park, 2014; Ko, Kim, & Hong, 2012; Muhammad et al., 2010; Tanaka, Matsumoto, & Shimoyama, 2007). Several studies were recently carried out on wings of Orthoptera (Wootton, Evans, Herbert, & Smith, 2000), Lepidoptera (O'Hara & Palazotto, 2012), Coleoptera (Sun et al., 2014; Zhang et al., 2018), and Odonata (Appel, Heepe, Lin, & Gorb, 2015; Li et al., 2014; Rajabi et al., 2016a, 2016b). Scientists proposed interesting novel models that make better structure performance inspired by beetles, especially the structure of the wings which can be used in industrial applications (Sun & Bhushan, 2012). Another important novel is related to the structure of the wing of Ladybird beetle which lead to the design of flapping wing micro air vehicle, this include small size and ability to fold when not in use, and this lead to the studying of the surface morphology and microstructure of the wings using SEM, atomic force microscope (AFM), and FTIR which was reported by Xiang, Du, & Zhen, 2016.

The elytra of Coleoptera have an ingenious structure with superhydrophobic characteristics, a structural coloration and anti-adhesion characteristics (Pfau & Honomichl, 1979; Sun & Bhushan, 2012). Previous research indicated that the shape and size of trabeculae form the internal connection between dorsal and ventral surface of the elytra which are related to species of beetles (Xiang, Qing, Endo, & Iwamoto, 2001). Besides that, Bouchard & Gorb, 2001 reported the morphological structure of the elytra on *Tabarus montanus* and detected the presence of a system of interlocking macrostructures to attach the elytra with the body. Noh, Muthukrishnan, Kramer, and Arakan (2016, 2017) reported the morphological and morphogenesis of the dorsal and ventral surface of the elytron of the red flour beetle *Tribolium castanaeum*. Also, Linz, Hu, Sitvarin, and Tomoyasu (2016) reported that there are little researches that demonstrated the significance function of the elytra of beetles and applying four stresses on the red flour beetle *Tribolium castanaeum*: physical damage to hindwings, predation, desiccation, and cold shock to show the importance of elytra. Zohry, 2017 reported the morphological structure of different stages of *Tribolium confusum* using scanning electron microscopy (SEM). Barbara & Piotr, 2017 reported that insect wing has two-layer membrane strengthened by longitudinal vein, cross vein, and supported by extracellular cuticle.

However, El-Kifl (1953) focused on the morphological differentiation in between *Tribolium castanaeum* and *T. confusum* the detailed structure of elytra and membranous wings of *Tribolium* species is not fully understood. The aim of the present work was to explore the

morphological and histological structure of dorsal and ventral surfaces of the fore and hindwings of *Tribolium castanaeum* and *T. confusum*. Also, this work explores the microstructure of the wings and their corresponding surface chemistry of both species using Fourier Transformed Infrared Spectroscopy (FTIR). Results obtained from this work may assist other efforts of researchers to make novel wing models which can be used in industrial applications that make better structure performance inspired by beetles and investigate the natural diversity in the properties of the wings of beetles.

Materials and methods

Insects

Insects used in this study were obtained from laboratory colonies reared on wheat flour at the Entomology laboratory at a constant temperature of 27 ± 2 and 70 ± 5 R.H., Faculty of Science, Sohag University, Egypt.

Scanning electron microscopy

The elytra and hindwings were collected from 40 beetles of *Tribolium castanaeum* and *T. confusum* in the laboratory and fixed in 70% alcohol. The samples were broken vertically with two fine forceps (Van de Kamp & Greven, 2010). The pieces were prepared for examination by subjecting them to dehydration series of 90%, 95% and absolute alcohol. Specimens were then critically point dried and coated with gold using sputter coating for examination using scanning electron microscope (SEM), JEOL, JSM 5300.

Light microscopy

For light microscopy studies; the pieces of elytra were immersed in 2.5% glutaraldehyde and in 0.1 M cacodylate buffer at 4 °C for 6 h. After washing in cacodylate buffer, the samples were post-fixed in 1% osmium tetroxide in 0.1 M cacodylate buffer at 4 °C for 2 h, rinsed in the same buffer. Dehydration in ethanol, then propylene oxide, was used in infiltration and was embedded in epon-araldite medium. Semi-thin sections were made with glass knife by Richert supernova ultratome and were stained by toluidine blue, then were examined under a light microscope.

Fourier transformed infrared spectroscopy

The distribution of organic functional groups on the forewing and hindwing of both *T. castanaeum* and *T. confusum* were analyzed using Fourier transformed infrared spectroscopy (FTIR, Switzerland). The samples were scanned in transmission mode using a Burker alpha platinumium ATR spectrometer. Absorption spectra were collected in the region between 3500 and 500 Cm^{-1} .

Results

Scanning electron microscopy

Forewing surface

Elytra of *T. castanaeum* were movably articulated with the mesothorax. The articular part of the elytron was a root, the small process which protrudes from the basal rim of the elytron (Fig. 1b). The maximum length and width of the forewing of *T. castanaeum* were 2.4 mm and 0.55 mm and for *T. confusum* were 2.37 mm and 0.79 mm respectively (Fig. 1a–d). Hexagonal structure with numerous gland opening was seen under SEM over the dorsal surface of the elytra. Each gland opening was found in a pit and each with a curved trichoid sensillum. Pits were common and randomly distributed on the surface of the forewing. The external element of the sensillum covers the gland opening or located next to it. Pits' shape was nearly circular, and the diameter range from 10.91 to 14.55 μm (Fig. 2a–c) for *T. confusum*. Pits' shape was circular or nearly oval and the diameter range from 7.0 to 10.0 μm (Fig. 2d–f). The number of pits was 28 per $184 \times 184 \mu\text{m}^2$ for *T. castanaeum* and 33 per $184 \times 184 \mu\text{m}^2$ for *T. confusum*. The distance between pits ranged from 20 to 39.47 μm and from 11.0 μm to 27.0 μm for *T. confusum* (Table 1). There was a rectangular convex in every pit at the apex of the forewing of both *T. castanaeum* and *T. confusum*; the length and width of the rectangular convex were 9.52 μm and 7.62 μm and 9.52 μm and 4.76 μm , respectively (Fig. 2c, f and Table 1). Microtrichia were found on the anterior

part of the ventral side of the elytron but the shape of the microtrichia in *T. castanaeum* was rectangular (Fig. 3a) and for *T. confusum* forming cone shape (Fig. 3b). Also, close to their posterior border, the later fields were covered by long spines for both two species (Fig. 4a, b).

Hindwing surface

SEM images of the surface along hindwing membrane of *T. castanaeum* and *T. confusum* indicate that the hindwing composed of three layers, which were referred to as the upper surface, the medium layer, and the lower surface (Fig. 5a–d). The upper and lower layers were both found to be composed of numerous spikes (Fig. 5a–d). These spikes were randomly distributed and vertical on the surface of the membranes (Fig. 5a–d). The distance between adjacent spikes for *T. castanaeum* ranged from 6.19 to 7.62 μm and the height of the spikes ranged from 0.9 to 1.85 μm . The number of spikes was 20 per $33 \times 33 \mu\text{m}^2$. The thickness of the medium layer for *T. castanaeum* was 1.11 μm (Fig. 5a, b and Table 1).

The distance between adjacent spikes for *T. confusum* ranged from 4.76 to 7.14 μm , and the height of the spikes ranged from 1.85 to 2.41 μm . The number of spikes was 23 per $33 \times 33 \mu\text{m}^2$. The thickness of the medium layer for *T. confusum* is 0.37 μm (Fig. 5c, d; Table 1).

Cross section of the forewing

A cross section of the forewing for both *T. castanaeum* and *T. confusum* was divided into three parts which

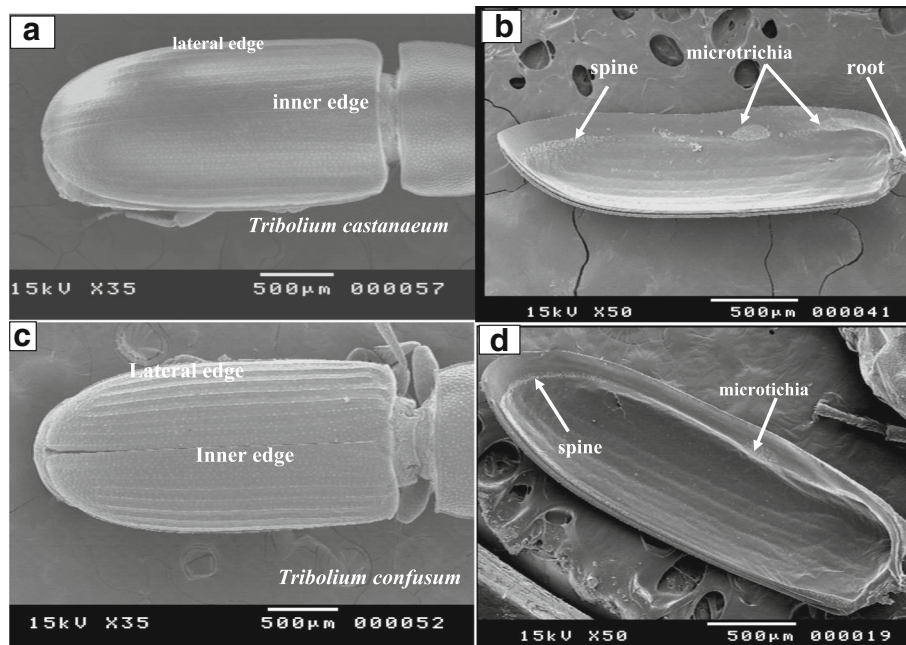


Fig. 1 Scanning electron microscope (SEM) images of *Tribolium* elytral morphology. **a** dorsal view and **b** ventral view *Tribolium castanaeum*. **c** dorsal view and **d** ventral view *Tribolium confusum*

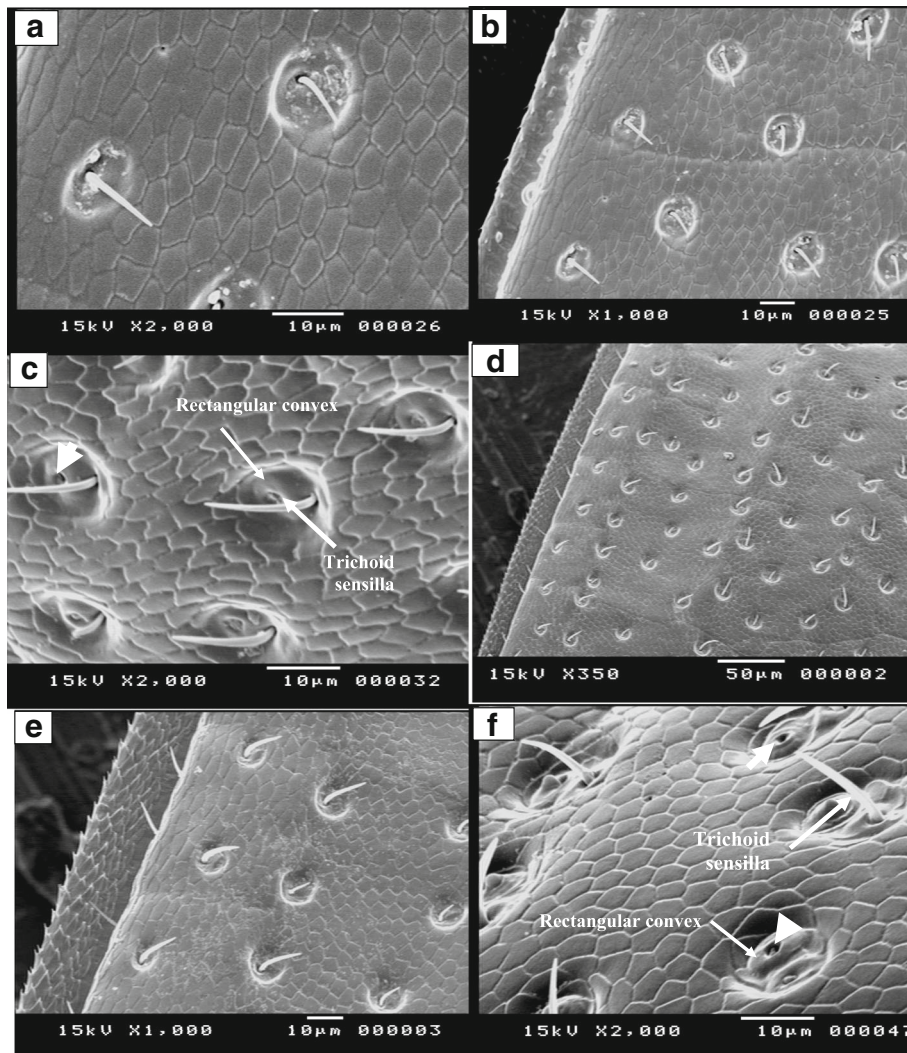


Fig. 2 Scanning electron microscope (SEM) images of elytral microstructure, dorsal surface of **a–c** *Tribolium castaneum* and **d–f** *Tribolium confusum* showing the opening of gland (head arrow) and trichoid sensilla

were the inner edge, the middle part, and the lateral edge (Fig. 6). The forewing consists of two halves joined by a series of connectors called trabeculae (Fig. 6). Dorsal (upper) and ventral (lower) parts of an elytron were separated by hemolymph space created by cuticular columns, the trabeculae. The thickness of the total elytra varied considerably across *T. castaneum* and *T. confusum* but also in different regions of an elytron. Further, the ventral cuticle was always thinner than the dorsal one (Fig. 6). Results showed that the thickness of the lateral edge, the middle part, and the inner edge of *T. castaneum* was 54.54 μm , 27.0 μm , and 38 μm , respectively (Table 1). The height of the hemolymph space lateral edge, the middle part, and the inner edge was 30.0 μm , 9 μm , and 16 μm , respectively (Fig. 6a, c, g, e; Table 1).

The thickness of the lateral edge, the middle part, and the inner edge of *T. confusum* was 53.75 μm , 22.70 μm , and 38.0 μm , respectively. The height of the hemolymph space lateral edge, the middle part, and the inner edge was 18.75 μm , 4.55 μm , and 12.5 μm , respectively (Fig. 6b, d, f, h and Table 1).

Semithin cross section on the forewing of *T. castaneum* and *T. confusum* shows that the height and width of the hemolymph space was extremely variable (Fig. 7a, b).

Cross sections of the hindwing

The hindwings of both *T. castaneum* and *T. confusum* composed of veins and membrane (Fig. 5a–d). The thickness of the membrane was approximately 1.11 μm for *T. castaneum* and 0.37 μm for *T. confusum* (Fig. 5a–d;

Table 1 Showing the different characters of forwing and hindwing for *T. castanaeum* and *T. confusum*

| Species | Forewing | | | | | | Hindwing | | | | | | | | | | |
|-----------------------------|----------|---------|----------------|-----------------------|--|--------------------|---------------------------|--------------------------|-------------------------|-------------------------------|----------------------|----------------------------------|--|-------------|--------------|--------------|----|
| | Length | Width | Size of pits | Distance between pits | Number of pits per 184 × 184 μm ² | Rectangular convex | Thickness of lateral edge | Thickness of middle part | Thickness of inner edge | Height of the hemolymph space | Height of the spikes | Distance between adjacent spikes | Number of spikes per 33 × 33 μm ² | | | | |
| | | | | | | Length | Width | | | Lateral edge | Middle part | inner edge | | | | | |
| <i>Tribolium castanaeum</i> | 2.4 mm | 0.55 mm | 10.91–14.55 μm | 20–39.47 μm | 28 | 9.52 μm | 7.62 μm | 54.54 μm | 27.0 μm | 38 μm | 9 μm | 16 μm | 1.11 μm | 0.9–1.85 μm | 6.19–7.62 μm | 20 | |
| <i>Tribolium confusum</i> | 2.37 mm | 0.79 mm | 7.0–10 μm | 11–27 μm | 33 | 9.52 μm | 4.76 μm | 53.75 μm | 22.7 μm | 38 μm | 18.75 μm | 4.55 μm | 12.5 μm | 0.37 μm | 1.85–2.41 μm | 4.76–7.14 μm | 23 |

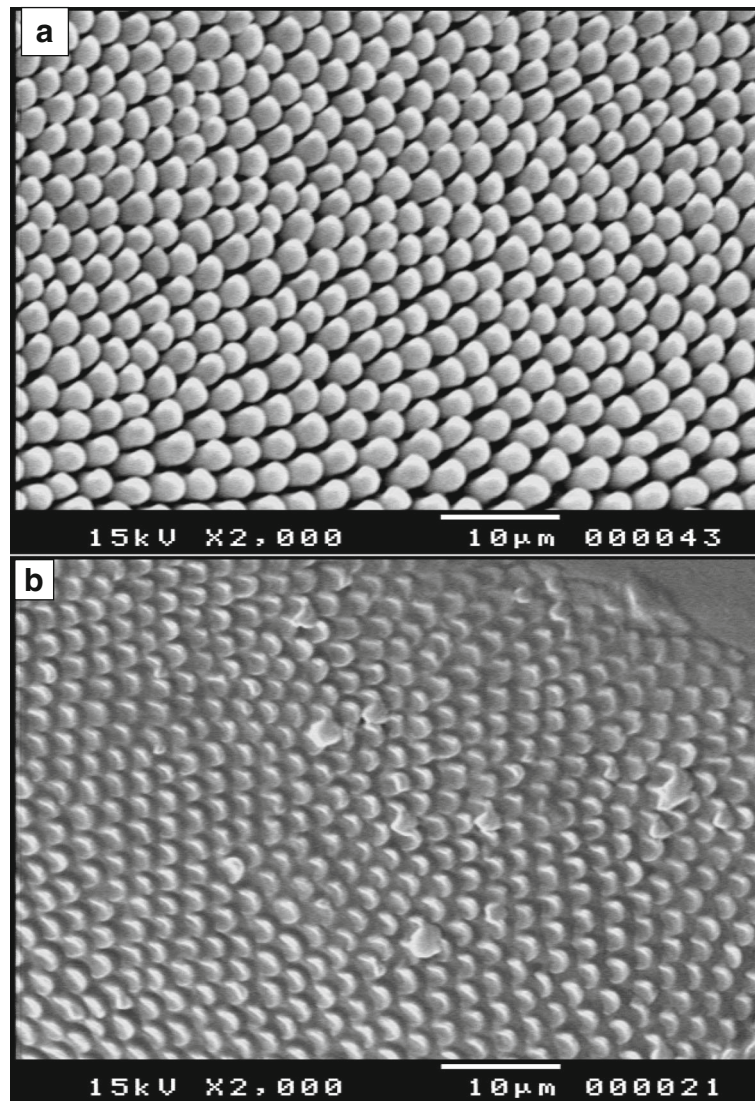


Fig. 3 Scanning electron microscope (SEM) images of microtrichia on the ventral surface of elytron of *Tribolium castanaeum* (a) and *Tribolium confusum* (b)

Table 1). Cross section of vein looks like a tubular structure (Fig. 5a–d).

Fourier transformed infrared spectroscopy

FTIR spectrum of the wings of T. castanaeum

The spectra from each forewing and hindwing were largely similar, containing three major band groups (Fig. 8a, c). The first group at $3301\text{--}3251\text{ cm}^{-1}$ corresponds to O–H, N–H stretching vibration. The second band group present at $2920\text{--}2850\text{ cm}^{-1}$ represents alkyl hydrocarbons. And finally, the third band group at $1743\text{--}1705\text{ cm}^{-1}$ corresponds to ester and amide carbonyl groups. The spectra of the two wings were dominated by amide I and amide II absorption bands.

An ester carbonyl stretching band presents at ($1742\text{--}1743\text{ cm}^{-1}$) in the two wings recorded spectra. The C–H stretching region ($2920\text{--}2850\text{ cm}^{-1}$) represents the symmetric (Vs) and anti-symmetric (Vs) stretching vibrations of CH_2 and CH_3 functional groups.

FTIR spectrum of the wings of T. confusum

The two main components of the *T. confusum* forewing were chitin and glycoprotein from FITR spectrum (Fig. 8b, d). Two high wave number spectral regions at ($3466\text{--}3339\text{ cm}^{-1}$) and (at approximately 3267 cm^{-1}) represent hydrogen-bonded O–H and N–H amidic stretching vibration, respectively. The relatively sharp bands corresponding to the C–H stretching vibrations were record at 2922 cm^{-1} and 2853 cm^{-1} . The bands at

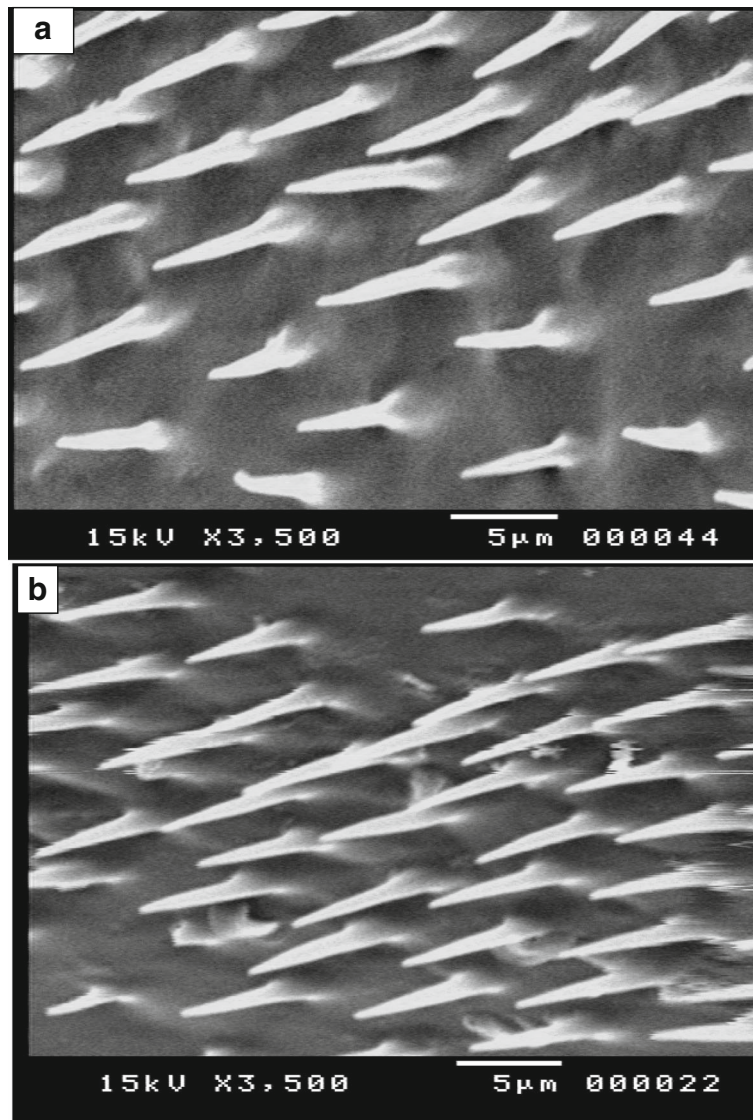


Fig. 4 Scanning electron microscope (SEM) images of spines on the ventral surface of elytron of *Tribolium castaneum* (a) and *Tribolium confusum* (b)

approximately (1652 cm^{-1} and 1623 cm^{-1}) are an (N–C=O) stretching vibration of the amide band which is present in chitin. The bands at 1151.38 cm^{-1} , 1113 cm^{-1} , and 951 cm^{-1} are C–N, C–O stretching vibration, and Cl–C bending vibration, respectively, which confirm the chitin structure. In addition, the bands of 1542 cm^{-1} and 1525 cm^{-1} indicate amino acid amide stretching vibrations which composed of different structures. The amino acid contains benzene ring confirmed by the presence of bands at 3105 cm^{-1} , 3084 cm^{-1} , 1447 cm^{-1} , and 1373 cm^{-1} . The coupled vibration peak that is composed of C–O, COO and C–O–C is at band of 1249 cm^{-1} , suggesting that glycoproteins exist in this structure.

The two main chemical components of the *T. confusum* hindwing were chitin and protein from FITR spectrum, as

shown in (Fig. 8b, d). The high wave number spectral region represents O–H stretching vibration, which occurred at 3467 cm^{-1} and 3407 cm^{-1} while bands at 3298 cm^{-1} and 3265 cm^{-1} represent N–H amidic stretching vibration. The relatively sharp and dense bands corresponding to the C–H stretching vibration were recorded at 2919 cm^{-1} and 2849 cm^{-1} . The bands at approximately 1655 cm^{-1} and 1628 cm^{-1} (N–C=O) stretching vibration of the amide band which present in chitin. The bands at 1153 cm^{-1} and 1065 cm^{-1} were C–O–C stretching vibration. The weak band approximately 873 cm^{-1} was a bending vibration of Cl–C.

Discussion

Over the total dorsal surface of the elytra of both *T. castaneum* and *T. confusum*, numerous gland openings

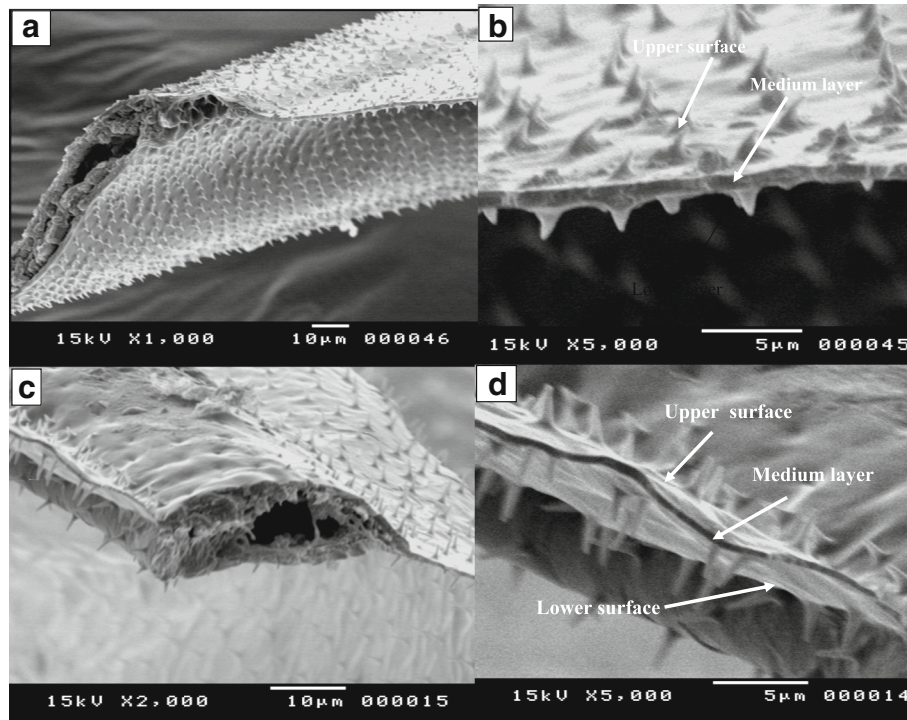


Fig. 5 Scanning electron microscope (SEM) images of cross section of hindwing of **a, b** *Tribolium castaneum* and **c, d** *Tribolium confusum*

were seen under SEM. Each gland opening was found in a pit and each with a curved trichoid sensillum. These results run parallel with other studies that reported the presence of glands distributed among sensilla of the cuticle in both male and female that they could play a role in mutual attraction of both sexes (Babier, Ferran, Le Lannic, & Allo, 1992; Faustini, Burkholder, & Laub, 1981; Francke, Levinson, Jen, & Levinson, 1979; Levinson et al., 1978; Levinson, Levinson, & France, 1981).

The present study showed the presence of a special structure called microtrichia on the ventral surface of the elytra of both *T. castaneum* *T. confusum*. The mechanical function of microtrichial fields is usually to fix one part of the body to another or to attach an organism to different substrates (Gorb, 1999; Hepburn, 1985; Richards & Richard, 1979). Also, the flying beetle closed their elytra to the body using locking devices, and these structures are supported by microtrichial fields in the inner surface of elytra and adjacent parts of the pterothorax (Gorb, 1999).

Elytra of beetles are lightweight and have multifunctional structures (Van de Kamp & Greven, 2010; Neville, 1993; De Souza & Alexander, 1997). They play a vital role like a composite material with a high resistance to bending and pressure, and to protect the hindwings and the body, and produce significant aerodynamic forces in those beetles which fly with their elytra expanded laterally.

The light-weight construction of elytra may be due to reducing their overall dorsal and ventral cuticle thickness, and the increasing of the hemolymph space. This was reported during this study for the elytra of *T. confusum* which is not flying and exhibits relatively small hemolymph spaces compared with the flying species *T. castaneum*. These results agree with that reported by Van de Kamp and Greven (2010) for three species which are flightless and exhibit relatively small hemolymph spaces (*Pterostichus niger*; *Trigonopterus nasutus*, *Sitophilus granarius*) and five species, which can fly having relatively large hemolymph space (*Cetonia aurata*, *Anoplotrupes stercorosus*, *Tenebrio molitor*, *Ceutorbynchus pallidactylus*, *Phyllobius betulinus*).

Pits were common and randomly distributed on the surface of the elytra for both *T. castaneum* and *T. confusum*. The dermal gland present on the elytra secretes a substance which may play an important role in hydrophobic characteristics. Similar explanation was also made by Sun & Bhushan, 2012. SEM of the elytron surface of *Coccinella septempunctata*, showed many shallow oval pits and existence of several hollow holes in the middle of the lateral and inner edges, which decrease weight and provide mechanical support (Xiang, Du, & Zhen, 2016).

The presence of spikes with different diameter (10–15 µm) and different heights (8–10 µm) on the hindwing, have been suggested to be important for contributing to its hydrophobic characteristics (Xiang, Du, & Zhen, 2016).

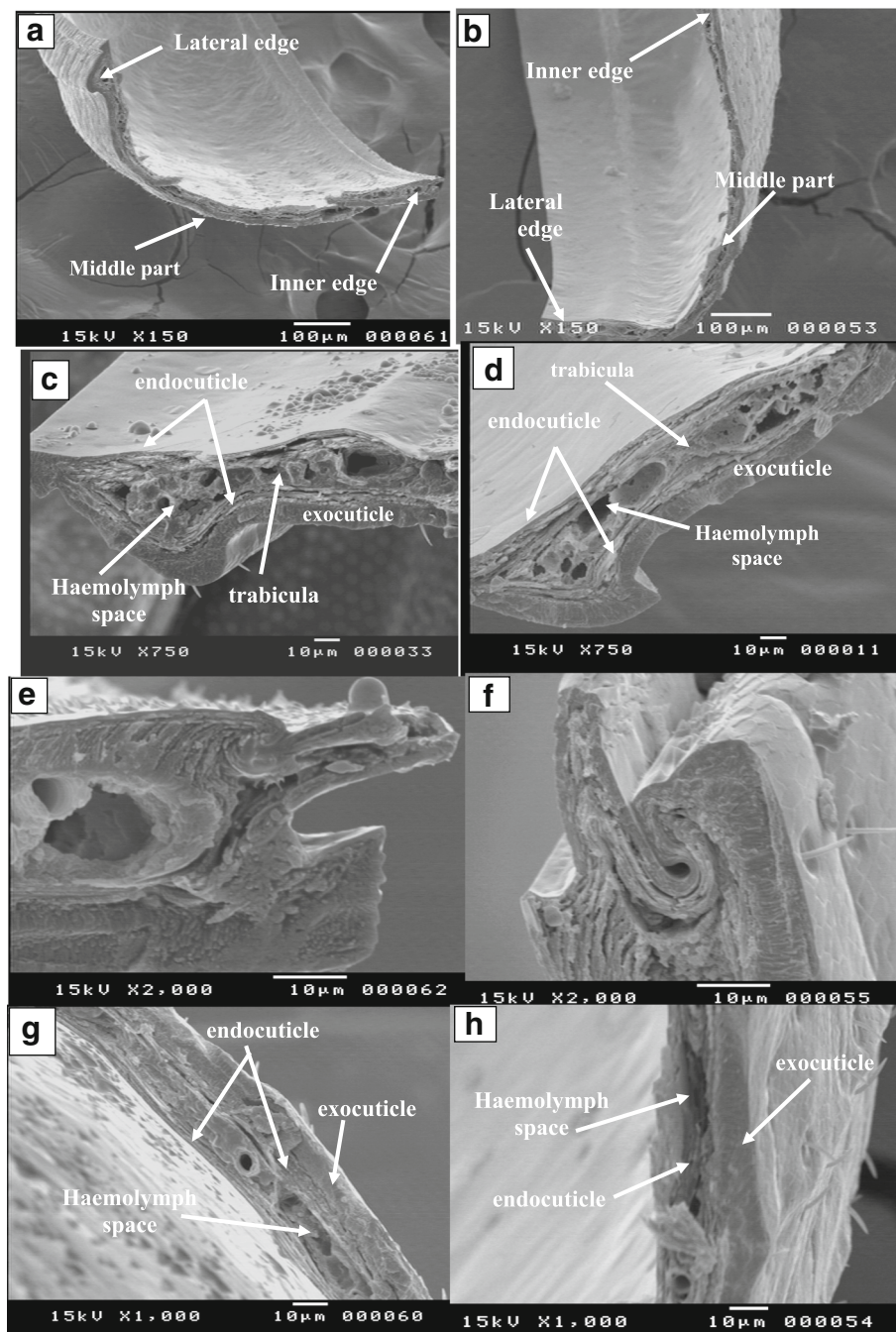


Fig. 6 Scanning electron microscope (SEM) images of cross section of elytron of (a, c, e, g) *Tribolium castaneum*; (a) whole cross section, (c) lateral edge, (e) inner edge, (g) middle part; (b, d, f, h) *Tribolium confusum*; (b) whole cross section, (d) lateral edge, (f) inner edge, (h) middle part, showing dorsal (upper) and ventral (lower) parts of elytrons were separated by haemolymph space created by trabeculae, the thickness of the elytrons are different among two species

In our study, the chemical function groups in the forewing and hindwing of *T. castaneum* were O–H, N–H stretching vibration, alkyl hydrocarbons, and ester and amide carbonyl group. Amide I and amide II were due to C=O band stretching coupled to N–H banding and C–N stretching coupled to N–H banding. The presence

of amide group can be attributed to the chitin and protein components of the wings, as they represent the major structural components that make up the bulk of the studying insect.

The presence of C–H stretching bands with the prevalence of methylene bands was an indication of

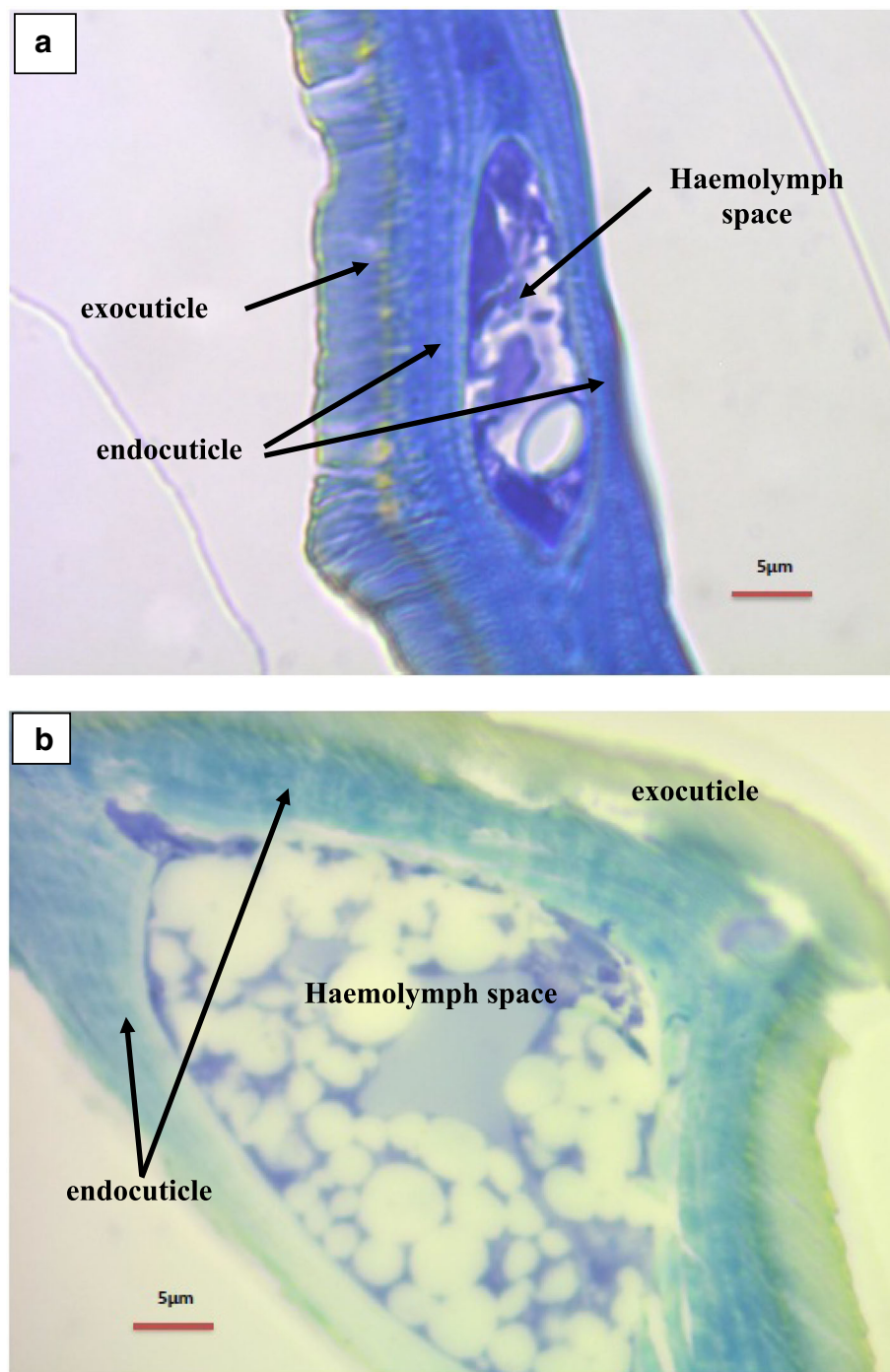


Fig. 7 Semi cross section of forewing of *Tribolium* sp. (a) *Tribolium confusum* (b) *Tribolium castanaeum*, showing thickness of exocuticle, endocuticle & the height of the haemolymph space

the presence of long-chain aliphatic acids in surface waxes.

The chemical components of the hindwing of *T. confusum* suggest that chitin exists in this structure. The strong peaks at 1544 cm^{-1} and 1517 cm^{-1} were caused by an amino acid, amide stretching vibration.

The amino acid that contained benzene ring shows bands between 1451 cm^{-1} and 1373 cm^{-1} were found in the structure. The coupled vibration peak that is composed of C–O, COO, and C–O–C was in a band at 1241 cm^{-1} and caused by the coupled vibration of chitin and protein. In sum, most of the hindwing was

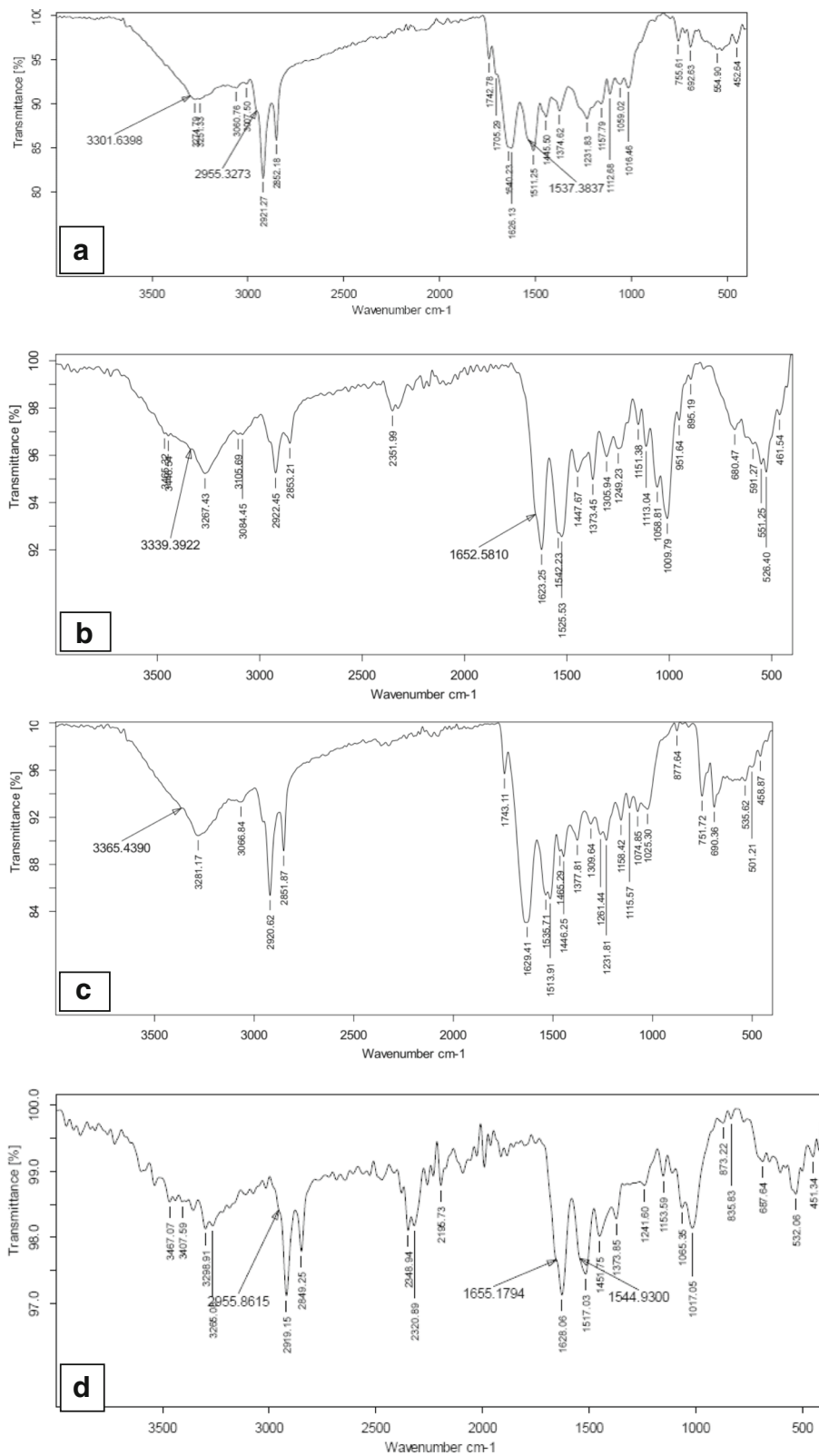


Fig. 8 IR absorbance spectra of the wings of **a, c** *Tribolium castaneum*—**a** elytron, **c** hindwing; **b, d** *Tribolium confusum*—**b** elytron, **d** hindwing

composed of chitin and contains small amount of other protein.

All samples contained protein/chitin components. But the presence of ester carbonyl stretching vibration bands at (1742–1743 cm^{-1}) in the two wings recorded spectra of *T. castanaeum*. The C–H stretching region (2920–2850 cm^{-1}) which represented the symmetric (Vs) and anti-symmetric (Vs) stretching vibrations of CH_2 and CH_3 functional groups with prevalence of methylene bands was an indication of the presence of long-chain aliphatic acids in surface waxes in *T. castanaeum*. This constituent showed that none wetting of these wings is due to the presence of cuticular waxes in *T. castanaeum*; these results agree with that reported by Nguyen et al. (2014) for dragonflies.

Conclusion

In this study, the natural diversity in the properties of the wings of *T. castanaeum* and *T. confusum* were studied. The results included Scanning electron microscopical structure of the forewing and hindwing of both *T. castanaeum* and *T. confusum*. The main findings were the presence of glandular openings, the hexagonal structure, and the rectangular convex which are like bumps that were common and randomly distributed on the dorsal surface of the forewing for both *T. castanaeum* and *T. confusum* and each with curved trichoid sensillum that would establish the surface energy and wetting properties. Also, there was a special structure called microtrichia found on the ventral surface of the elytra. The thickness of the elytra was variable among different regions between the two *Tribolium* species; the surface structure along hindwing membrane indicated that there is a composite of three layers, which are the upper surface, the medium layer, and the lower surface. The upper and lower layers were both found to contain numerous spikes. These spikes are randomly distributed and vertical on the surface of the membranes where the length of these spikes in *T. confusum* is nearly twice in heights as *T. castanaeum*. Further investigation of chemical properties of these insect wings may lead to a greater understanding of the presence of cuticular waxes on both fore and hindwing of *T. castanaeum* to protect them from wetting.

Acknowledgements

I would like to express my thanks to the SEM unit, Assuit University for their efforts in specimen preparation.

Funding

Not applicable.

Availability of data and materials

Data for Entomology branch.

Authors' contributions

NM is the main author for the manuscript. AME-S is the second author. Both authors read and approved the final manuscript.

Ethics approval and consent to participate

All experiments were done according to the guidance and animal care ethics of Sohag University, Egypt.

Consent for publication

I agree to the publication.

Competing interests

The authors declare that they have no competing interests.

Publisher's Note

Springer Nature remains neutral with regard to jurisdictional claims in published maps and institutional affiliations.

Author details

¹Department of Zoology, Faculty of Science, Sohag University, Sohag, Egypt.

²Department of Chemistry, Faculty of Science, Sohag University, Sohag, Egypt.

Received: 3 September 2018 Accepted: 24 January 2019

Published online: 05 March 2019

References

- Appel, E., Heepe, L., Lin, C.-P., & Gorb, S. N. (2015). Ultrastructure of dragonfly wing veins: Composite structure of fibrous material supplemented by resilin. *Journal of Anatomy*, 227, 561–582.
- Babier, B., Ferran, A., Le Lannic, J., & Allo, M. R. (1992). Morphology and ultrastructure of integumentary glands of *Semiadalia undecimnotata* SCHN. (Coleoptera: Coccinellidae). *International Journal of Insect Morphology and Embryology*, 3(21), 223–234.
- Barbara, F. P., & Piotr, W. (2017). The fore wing of the *Apis fabae* (Scopoli 1763) (Hemiptera, Sternorrhyncha): A morphological and histological study. *Zoomorphology*, 136(3):349–358.
- Bouchard, P., & Gorb, S. N. (2001). The elytra-to-body binding mechanism of the flightless rainforest species *Tabarus montanus* Kaszab (coleopteran: Tenebrionidae). *Arthropod Structure & Development*, 29, 323–331.
- De Souza, M. M., & Alexander, D. E. (1997). Passive aerodynamic stabilization by beetle elytra (wing covers). *Physiological Entomology*, 22, 109–115.
- El-Kifl, A. H. (1953). Morphology of the adult *Tribolium confusum* Duv. and its differentiation from *Tribolium* (Stene) *castaneum* Herbst. (Coleoptera: Tenebrionidae). *Bulletin de la Société Fouad Premier Entomology*, 37, 173–249.
- Faustini, D. L., Burkholder, W. E., & Laub, R. J. (1981). Sexual dimorphic setiferous puncture in the male red flour beetle, *Tribolium castaneum* Herbst (Coleoptera:Tenebrionidae): Site of aggregation pheromone production. *Journal of Chemical Ecology*, 7(2), 467–482.
- Francke, W., Levinson, A. R., Jen, T. L., & Levinson, H. Z. (1979). Isopropyl carboxylates. A new class insect pheromones. *Angewandte Chemie International Edition*, 18(10), 796–797.
- Gorb, S. N. (1999). Ultrastructure of the thoracic dorso-medial field (TDM) in the elytra –to– body arresting mechanism in Tenebrionid Beetles (Coleoptera: Tenebrionidae). *Journal of Morphology*, 240(2), 101–113.
- Ha, N., Truong, Q., Phan, H., Goo, N., & Park, H. (2014). Structural characteristics of *Allomyrina dichotoma* beetles hind wings for flapping wing micro air vehicle. *Journal of Bionic Engineering*, 11, 226–235.
- Hepburn, H. R. (1985). Structure of the integument. In G. A. Kerkut, & L. I. Gilbert (Eds.), *Comprehensive insect physiology, biochemistry, and pharmacology*, (pp. 1–58). Oxford: Pergamon, Press.
- Ko, J., Kim, J., & Hong, J. (2012). Micro/nanofabrication for a realistic beetle wing with a superhydrophobic surface. *Bioinspiration & Biomimetics*, 7, 016011.
- Levinson, A. R., Levinson, H. Z., & France, W. (1981). Intraspecific attractants of the hide beetle *Dermestes maculatus* (DeGeer). *Mitteilungen der Deutscher Gesellschaft für Allgemeine und Angewandte Entomologie*, 2(3/5), 235–237.
- Levinson, H. Z., Levinson, A. R., Jen, T. L., Williams, J. L. D., Kahn, G., & Francke, W. (1978). Production site, partial composition and olfactory perception of a pheromone in the male hide beetle. *Naturwissenschaften*, 65(10), 543–544.
- Li, X., Zhang, Z., Liang, Y., Ren, L., Jie, M., & Yang, Z. (2014). Antifatigue properties of dragonfly *Pantala flavescens* wings. *Microscopy Research and Technique*, 77, 356–362.
- Linz, D. M., Hu, A. W., Sitvarin, M. I., & Tomoyasu, Y. (2016). Functional value of elytra under various stresses in the red flour beetle, *Tribolium castaneum*. *Scientific Reports*, 6(34813), 1–10.

- Muhammad, A., Nguyen, Q., Park, H., Hwang, D., Byun, D., & Goo, N. S. (2010). Improvement of artificial foldable wing models by mimicking the unfolding/folding mechanisms of a beetle hind wing. *Journal of Bionic Engineering*, 7, 134–141.
- Neville, A. C. (1993). *Biology of fibrous composites development beyond the cell membrane*. Cambridge: Cambridge University Press.
- Nguyen, S. H., Webb, H. K., Hasan, J., Tobin, M. J., Mainwaring, D. E., Mohan, P. J., ... Grawford, R. J. (2014). Wing wettability of odonata species as a function of quality of epicuticular waxes. *Vibrational Spectroscopy*, 75, 173–177.
- Noh, M. Y., Muthukrishnan, S., Kramer, K. J., & Arakan, Y. (2016). Cuticle formation and pigmentation in the beetles. *Current Opinion in Insect Science*, 17, 1–9.
- Noh, M. Y., Muthukrishnan, S., Kramer, K. J., & Arakan, Y. (2017). Development and ultrastructure of the rigid dorsal and flexible ventral cuticle of the elytron of the red flour beetle, *Tribolium castaneum*. *Insect Biochemistry and Molecular Biology*, 91, 21–33.
- O'Hara, R. P., & Palazotto, A. N. (2012). The morphological characterization of the forewing of the *Manduca sexta* species for the application of biomimetic flapping wing micro air vehicles. *Bioinspiration & Biomimetics*, 7, 1–13. <https://doi.org/10.1088/1748-3182/7/4/046011>.
- Pfau, H. K., & Honomichl, K. (1979). Die campaniformen sensillen des flugels von *Cetonia aurata* L. und *Geotrupes silvaticus* panz. (insect, Coleoptera) in ihrer beziehung zur flugelmechanik and flugfunktion. *Zoologische Jahrbücher*, 102, 583–613.
- Rajabi, H., Rezasefat, M., Darvizeh, A., Dirks, J. H., Eshghi, S. H., Shafiei, A., ... Gorb, S. N. (2016). A comparative study of the effects of constructional elements on the mechanical behaviour of dragonfly wings. *Applied Physics A*, 122, 19. <https://doi.org/10.1007/s00339-015-9557-6>.
- Rajabi, H., Shafiei, A., Darvizeh, A., Dirks, J.-H., Appel, E., & Gorb, S. N. (2016). Effect of microstructure on the mechanical and damping behaviour of dragonfly wing veins. *Royal Society Open Science*, 3, 160006.
- Richards, A. G., & Richard, R. A. (1979). The cuticular protuberances of insects. *International Journal of Insect Morphology and Embryology*, 8, 143–157.
- Sun, S., & Bhushan, B. (2012). Structure and mechanical properties of beetle wings: A review. *RSC Advances*, 2(33), 12606–12623.
- Sun, J., Ling, M., Wu, W., Bhushan, B., & Tong, J. (2014). The hydraulic mechanism of the unfolding of hind wings in *Dorcus titanus platymelus* (order: Coleoptera). *International Journal of Molecular Sciences*, 15, 6009–6018. <https://doi.org/10.3390/ijms15046009>.
- Tanaka, H., Matsumoto, K., & Shimoyama, I. (2007). Fabrication of a three dimensional insect-wing model by micromolding of thermosetting resin with a thin elastmeric mold. *Journal of Micromechanics and Microengineering*, 17, 2485–2490.
- Van de Kamp, T., & Greven, H. (2010). On the architecture of beetle elytra. *Entomologie Beute*, 22, 191–204.
- Wootton, R. J., Evans, K. E., Herbert, R., & Smith, C. W. (2000). The hind wing of the desert locust (*Schistocerca gregaria* Forskål). I functional morphology and mode of operation. *Journal of Experimental Biology*, 203, 2921–2931.
- Xiang, J., Du, J., & Zhen, C. (2016). Functional morphology and structural characteristics of wings of the ladybird beetle, *Coccinella septempunctata* (L.). *Microscopy Research and Technique*, 79, 550–556.
- Xiang, J., Qing, N. Q., Endo, Y., & Iwamoto, M. (2001). Fine structure of trabeculae in the elytra of *Allomyrina dichotoma* (LINNE) and *Prosopocoilus Inclinator* (Motschulsky) (Coleoptera: Scarabaeidae). *Entomologia Sinica*, 2(8), 115–123.
- Zhang, S. Q., Che, L. H., Liang, D., Pang, H., Lipinski, A., & Zang, P. (2018). Evolutionary history of Coleoptera revealed by extensive sampling of genes and species. *Nature Communications*, 9(205), 1–11.
- Zohry, N. M. (2017). Scanning electron morphological studies of *Tribolium confusum* Jacquelin du Val (coleopteran: Tenebrionidae). *The Journal of Basic and Applied Zoology*, 78(1), 6.

Submit your manuscript to a SpringerOpen® journal and benefit from:

- Convenient online submission
- Rigorous peer review
- Open access: articles freely available online
- High visibility within the field
- Retaining the copyright to your article

Submit your next manuscript at ► [springeropen.com](https://www.springeropen.com)
